EFFECT OF SWIRL MOTION ON THE COFFICIENT OF FRICTION AND CONVECTIVE HEAT TRANSFER IN CIRCULAR ANNULI

Part(1) THEORETICAL ANALYSIS.

BY

Dr.M.B.MADY (1) Dr.B.A.KHALIFA(2) Dr.K.A.A.EL-SHORBAGY(3)

Eng.S.H.SHAMS EL-DIN(4)

ABSTRACT:

The coefficient of friction and heat transfer are studied for these condition of laminar swirling flow in the annular space between two Co-axial cylinders. Incompressible and steady flow conditions are considered. Computer solutions were found for the effect of annular gap height,injection angle and Reynolds number on the coefficients of friction and heat convection. The results show that,both the coefficient of friction and coefficient of heat transfer increase with increase in swirl angle, and decrease with decrease of gap width.

INTRODUCTION:

Swirl flow has a potential practical importance in many fields of industrial engineering. Numerous studies were devoted to understanding and declarations of the swirl generation condition on the friction and heat transfer parameters. Most of these studies deal with the turbulent swirling flow in pipes and in the annular space between two co-axial cylinders . One can mention among others those of Talbot [1] for laminar pipe flow . Fully developed turbulent flows with weak swirl components were analyzed theoretically by Kreith-Sonju [2] & Rochino-Lavan [3] ,also obtained a numerical solution for a turbulent swirling flow and change of axial velocity profile due to swirling motion was found by Yajinig -Subbaiah [4] to obey the velocity defect law applicable to turbulent parallel flow .Seno [5] studied experimentally the effects of wall roughness on the decay of swirl flows in a long circular pipe .

Concerning the annular space flow,Taylor [6] investigated fully developed rotating turbulent flow between concentric rotating cylinders. Rask-Scott [7] studied a developing axial

---

1)Prof. Faculty of Engineering Alexandria University.
2)Ass.Prof. Faculty of Engineering&Tech. Menoufia University.
3)Ass.Prof.Faculty of Engineering - Alexandria University.
4)Demonstrator,Faculty of Eng.&Tech.Menoufia University.

and decaying tangential velocity fields in a stationary annulus with a nearly free vortex initial velocity distribution . Isothermal air was used as the working fluid in an annulus,with a single diameter ratio($di/d_o = 0.4$) and at a single axial bulk Reynolds number of 1.3×10^5 . Simmers -Coney [8]studied the effect of Taylor vortex flow on the development length in concentric annuli.

The effect of gap width and swirl angle of unguided swirl flow in the annular space between two-co-axial cylinders on coefficient of friction and heat transfer needs further study.
In this paper the steady ,swirling,axially symmetric and Incompressible ,laminar flow in the annular space between two co-axial cylinders is considered theoretically.

NOMENCLATURE:

C_p Specific heat at constant pressure.
d_e Equivalent diameter of annulus, $[2(r_2'-r_1')]$.
d_i Diameter of inner cylinder .
d_o Diameter of outer cylinder .
f Coefficient of friction .
h Coefficient of heat transfer .
k Thermal conductivity of fluid .
N Annular radius ratio, (r_1'/r_2').
N_u Nusselt number, $(h.de/k)$.

P' Pressure .
P Dimensionless pressure, $(P_o-P')/\rho \bar{w}^2$.
P_r Prandtl number, $(\mu Cp/k)$.

q Quantity of heat transfer .
r_1' Radius of inner annular surface .
r_2' Radius of outer annular surface .

R_e Reynolds number, $(\bar{w}.d_e/\nu)$.
r', θ, Z' Cylinderical polar coordinates .
r, Z Dimensionless variables $r = r'/r_2'$, $Z = z'/r_2'$.
T' Temperature.
T Dimensionless temperature, T'/T_s.

T_b' Bulk temperature, $\int_{r_1'}^{r_2'} Tw' r' dr' \Big/ \int_{r_1'}^{r_2'} w' r' dr'$.

ΔT_w Drop of temperature on the wall.
T_s Temperature of surrounding .
u', v', w' Velocity components in the direction of r', θ, z' .

u, v, w	Dimensionless velocity components, $u=\dot{w}/\bar{w}$, $V = \dot{v}/\bar{w}$, $w = \dot{w}/\bar{w}$.
$\bar{W}$	Axial mean velocity .
α	Injection angle .
μ	Dynamic viscosity .
ν	Kinematic viscosity .
ρ	Density .

Governing equations

In order to predict fricitional losses and heat transfer rates in an unguided laminar swirl flow, the fundamental equations necessary describe the motion are the equation of continuity and Navier-Stokes equations. The heat transfer treatment, the thermal energy equation is to be added . In the case of a steady and rotationally symmetrical laminar flow, these equations can be written as :

$$\frac{\partial(\dot{r}\,\dot{u})}{\partial\dot{r}} + \frac{\partial(\dot{r}\,\dot{w})}{\partial\dot{z}} = 0 \quad \ldots\ldots\ldots\ldots \text{(1-a)}$$

$$\frac{\dot{u}\,\partial\dot{u}}{\dot{r}} - \frac{\dot{v}^2}{\dot{r}} + \dot{w}\frac{\partial\dot{u}}{\partial\dot{z}} = -\frac{1}{\rho}\frac{\partial\dot{p}}{\partial\dot{r}} + \nu\left(\nabla^2 u - \frac{\dot{u}}{\dot{r}^2}\right) \ldots \text{(1-b)}$$

$$\frac{\dot{w}\,\partial\dot{v}}{\partial\dot{r}} + \frac{\dot{u}\,\dot{v}}{\dot{r}} + \dot{w}\frac{\partial\dot{v}}{\partial\dot{z}} = \nu\left(\nabla^2\dot{v} - \dot{v}/\dot{r}^2\right) \ldots\ldots\ldots \text{(1-c)}$$

$$\dot{u}\frac{\partial\dot{w}}{\partial\dot{r}} + \dot{w}\frac{\partial\dot{w}}{\partial\dot{z}} = -\frac{1}{\rho}\frac{\partial\dot{p}}{\partial\dot{z}} + \nu\nabla^2\dot{w} \ldots\ldots\ldots \text{(1-d)}$$

$$\rho C_p\left(\dot{u}\frac{\partial\dot{T}}{\partial\dot{r}} + \dot{w}\frac{\partial\dot{T}}{\partial\dot{z}}\right) = K\nabla^2\dot{T} \quad \ldots\ldots\ldots\ldots \text{(1-e)}$$

Where, $\nabla^2 = \dfrac{\partial^2}{\partial\dot{r}^2} + \dfrac{1}{\dot{r}}\dfrac{\partial}{\partial\dot{r}} + \dfrac{\partial^2}{\partial\dot{z}^2}$

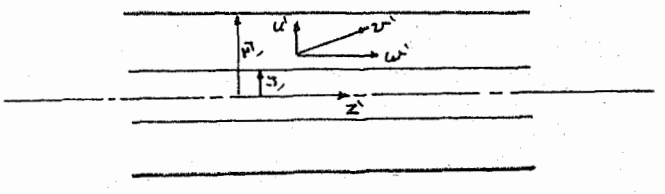

Fig.(1)Coordinate system.

The flow configuration is shown in Fig.(1), in which $\dot{Z}$ corresponds to the axial direction. At the inlet section $\dot{w} = \bar{w}\,f(\dot{r})$, $\dot{v} = \bar{w}g\,(\dot{r})$ and $\dot{T} = T_s h(\dot{r})$. The functions $f(\dot{r})$,

$g(\hat{r})$ define the distribution of velovity in the axial and tangential direction, respectively and $h(\hat{r})$ designates the temperature profile. Making use of these variables, one introduces the dimensionless variables and parameters as follows :

$$r = \hat{r}/\hat{r}_2 , \quad Z = \hat{z}/\hat{r}_2 , \quad N = \hat{r}_1/\hat{r}_2 , \quad u = \hat{u}/\bar{w}, \quad v = \hat{v}/\bar{w}, \quad w = \hat{w}/\bar{w} ,$$

$$P = (P_o - \hat{P})/\rho \bar{w}^2 , \quad T = \hat{T}/T_s , \quad Re = 2 \bar{w} \hat{r}_2 (1-N)/\nu \text{ and } Pr = \frac{\mu Cp}{k} .$$

In the work under consideration on order of magnitude analysis shows that the radial velocity($\hat{u}$)is much smaller than the tangential and axial velocities ($\hat{v}$,$\hat{w}$).Rewriting Eqs: (1-a) to (1-e) in terms of the above dimensionless variables and applying the boundary layer approximation the resulting equations are obtained:

$$\frac{\partial (r\,u)}{\partial r} + \frac{\partial (r\,w)}{\partial z} = 0 \qquad \ldots\ldots\ldots (2\text{-a})$$

$$- v^2/r = - \partial P/\partial r \qquad \ldots\ldots\ldots (2\text{-b})$$

$$u \frac{\partial u}{\partial r} + \frac{u\,v}{r} + w \frac{\partial v}{\partial z} = \frac{2(1-N)}{Re} \left(\frac{\partial^2 v}{\partial r^2} + \frac{1}{r} \frac{\partial v}{\partial r} - \frac{v}{r} + \frac{\partial^2 v}{\partial Z^2} \right) \ldots (2\text{-c})$$

$$u \frac{\partial w}{\partial r} + w \frac{\partial w}{\partial Z} = - \frac{\partial P}{\partial Z} + \frac{2(1-N)}{R_e} \left(\frac{\partial^2 w}{\partial r^2} + \frac{1}{r} \frac{\partial w}{\partial r} + \frac{\partial^2 w}{\partial Z^2} \right) \qquad (2\text{-d})$$

$$\frac{u \partial T}{\partial r} + w \frac{\partial T}{\partial z} = \frac{2(1-N)}{Re \cdot Pr} \left(\frac{\partial^2 T}{\partial r^2} + \frac{1}{r} \frac{\partial T}{\partial r} + \frac{\partial^2 T}{\partial Z^2} \right) \ldots (2\text{-e})$$

The continuity equation in the integral dimensionless form is :

$$\int_N^1 w r \, \partial r = \tfrac{1}{2} (1 - N^2) \qquad \ldots\ldots\ldots (2\text{-f})$$

The boundary conditions are :

At $Z = 0$ $v = g(r)$, $w = f(r)$, $T = h(r)$, and $P = 0$
At $Z \gg 0$ and $r = N$, $u, v, w = 0$, and $\Delta T w$ = constant
at $Z \gg 0$ and $r = 1$, $u, v, w = 0$, and $q = 0$

Equations (2-a) to (2-e) are nonlinear partial differential equations and obviously there exists no analytical solution for such equations, under the above mentioned boundary conditions which are valid throughout the decaying swirl length .

Thus, in order to obtain a solution for Eqs.(2-a)to (2-e), one would have to employ a perturbation method or an appropriate linearization technique for the inertia terms . These procedures would necessarily introduce some errors in the resulting solutions which can not be estimated unless the exact solutions are found . Accordingly a finite difference method (Appendix (A) was used to solve these equations . In terms of finite differences these equations read :

$$U_{j+1,k+1}=U_{j+1,k}\left[\frac{N+(k-1)\,\Delta R}{N+k\,\Delta R}\right]-\frac{\Delta R}{4\Delta Z}\left[\frac{2N+(2k-1)\,\Delta R}{N+k\,\Delta R}\right]\left[W_{j+1,k+1}+W_{j+1,k}-W_{j,k+1}-W_{j,k}\right] \quad \ldots (3\text{-a})$$

$$\frac{v^2_{j+1,k}}{N+(k-1)\,\Delta R}=\frac{P_{j+1,k}-P_{j+1,k-1}}{\Delta R} \quad \ldots\ldots\ldots (3\text{-b})$$

$$C_1\,v_{j+1,k-1}+C_2\,v_{j+1,k}+C_3\,v_{j+1,k+1}=C_4 \quad \ldots\ldots (3\text{-c})$$

$$-\frac{P_{j+1,k}}{\Delta Z}+C_1\,W_{j+1,k-1}+C_5\,W_{j+1,k}+C_3\,W_{j+1,k+1}=C_6 \quad \ldots (3\text{-d})$$

$$C_7\,T_{j+1,k-1}+C_8\,T_{j+1,k}+C_9\,T_{j+1,k+1}=C_{10} \quad \ldots\ldots (3\text{-e})$$

and the integral continuity equation(2-f) reduces to

$$\Delta R\sum_{k=2}^{n} R(k)\,W_{j+1,k}=\tfrac{1}{2}(1-N^2) \quad \ldots\ldots\ldots (3\text{-f})$$

Where

$$C_1=\frac{u_{j,k}}{2\,\Delta R}+\frac{2(1-N)}{Re\,\Delta R^2}-\frac{(1-N)}{Re\,R(k)\,\Delta R}$$

$$C_2=\frac{2(1-N)}{Re\,\Delta Z^2}-\frac{W_{j,k}}{\Delta Z}-\frac{4(1-N)}{Re\,\Delta R^2}-\frac{U_{j,k}}{R(k)}-\frac{2(1-N)}{Re\,R^2(k)}$$

$$C_3=\frac{(1-N)}{Re\,R(k)\Delta R}+\frac{2(1-N)}{Re\,\Delta R^2}-\frac{u_{j,k}}{2\,\Delta R}$$

$$C_4 = \frac{4(1-N)}{Re\,\Delta Z^2} V_{j,k} - \frac{W_{j,k}\,V_{j,k}}{\Delta Z} - \frac{2(1-N)}{Re\,\Delta Z^2} V_{j-1,k}$$

$$C_5 = -\frac{2(1-N)}{Re\,\Delta Z^2} - \frac{4(1-N)}{Re\,\Delta R^2} - \frac{W_{j,k}}{\Delta Z}$$

$$C_6 = -\frac{P_{j,k}}{\Delta Z} - \frac{W^2_{j,k}}{\Delta Z} + \frac{4(1-N)}{Re\,\Delta Z^2} W_{j,k} - \frac{2(1-N)}{Re\,\Delta Z^2} W_{j-1,k}$$

$$C_7 = \frac{(1-N)}{Re\,Pr\,R(k)\,\Delta R} - \frac{2(1-N)}{Re\,Pr\,\Delta R^2} - \frac{U_{j,k}}{2\,\Delta R}$$

$$C_8 = \frac{W_{j,k}}{\Delta Z} + \frac{4(1-N)}{Re\,Pr\,\Delta R^2} - \frac{2(1-N)}{Re\,Pr\,\Delta Z^2}$$

$$C_9 = \frac{U_{j,k}}{2\,\Delta R} - \frac{2(1-N)}{Re\,Pr\,\Delta R^2} - \frac{(1-N)}{Re\,Pr\,R(k)\,\Delta R} \quad , \text{and}$$

$$C_{10} = \frac{W_{j,k}\,T_{j,k}}{\Delta Z} + \frac{2(1-N)(T_{j-1,k} - 2\,T_{j,k})}{Re\,Pr\,\Delta Z^2}$$

K is the integral counter in the direction of (r)
J is the integral counter along the test section .

Equs. (3-b) ,(3-c) ,(3-d) and (3-f)are simultaneous linear algebraic equations, which can be solved numerically to obtain u , v , w and P. Supsitutautig the results of these quanties, at the end of a step; in Equ.(3-e), the temperature can be determined at the end of the step and thus the temperature distribution at a given section was obtained .

In order to predict the friction losses, the following equation is used : $$f = \frac{P_o - P'}{\rho \overline{W}^2} \frac{de}{Z} \quad \ldots\ldots \quad (4)$$

This equation can be written in the dimensionless form as:

$$f = -4P\,(1-N)/Z \quad \ldots\ldots\ldots\ldots \quad (5)$$

In this equation, P is the average dimensionless pressure over any cross section at a distance Z from the entrance:

$$\text{i.e. } P = \int_N^1 P_r dr \Big/ \int_N^1 r dr \quad \ldots\ldots\ldots\ldots (6)$$

HEAT TRANSFER CHARACTERISTICS:

The coefficient of heat transfer is defind by:

$$h(T_b - T_w) = -k(\partial T/\partial r)_{at\ r=r_1} \quad \ldots\ldots (7)$$

Where, T_b is the bulk temperature $= \int_{r=r_1}^{r=r_2} T w r\, dr \Big/ \int_{r_1}^{r_2} w r\, \partial r$

The bulk temperature in a dimensionless form is defined as :

$$T_b = \int_{N}^{1} T_w r dr \Big/ \int_{N}^{1} w r\, d r \quad \ldots\ldots\ldots (8)$$

The local Nusselt number (Nu) becomes:

$$N_u = \frac{d_e . h}{k} = \frac{d_e}{k} \cdot \frac{k(\partial T/\partial r)wall}{T_b - T_w}$$

or simply $N_u = -\frac{2(1-N)}{T_b(J) - T_w(J)} \frac{\partial T}{\partial r} \quad \ldots\ldots (9)$

Using Eqn (9) the local Nusselt number at any cross section at a given distance Z from the entrance can be calculated.

RESULTS AND DISCUSSION :

1-Tangential velocity:

Samples of the computed tangential and axial velocity profiles are shown in Figs (2,3,4). Fig.(2) shows the effect of swirl angle (α)on the tangential velocity distribution . It is clear that the increase of the angle (α) leads to an increase of the mean tangential velocity. This is expected since the rotating mass flux increases with the increase in swirl angle . The peak of the tangential velocity distribution is shifted gradually towards the inner wall as (α) increases . This can be a result of the increase of kinetic energy near the walls due to the increase of mass flux.Fig.(3) shows the effect of Reynolds number on the tangential velocity profiles. It can be seen that an increase in (Re) leads to an increase in V_{max} to a certain limit ($R_e \simeq 1000$) after which the increase in (R_e) leads to a decrease in V_{max}..

At small values of (Re) the increase of (R_e) increases the rotating mass flux,but at higher Reynolds number this leads to separation of flow. This would explain the apparent reduction in $V_{max.}$ at high Reynolds numbers .

Fig.(4) shows the effect of gap width. It is seen that a reduction in the gap width leads to increasing the mean tangential velocity . This is a result of the flow area . The smaller the gap width the smaller the area of flow and hence the higher the velocity. The shift of $V_{max.}$ towards the outer wall is due to the centrifugal force, which increases with the decrease of gap width.

2)Axial velocity:

The axial velocity profiles are shown in Figs(5 to7). Fig.(5) shows the effect of swirl angle on axial velocity variation across the annuli . As (α) increases the axial velocity increases at the inner wall side and decreases at the outer side . At high injection angles reverse flow is noticeable . The effect of (Re) is similar to that of (α) ,as can be seen from fig(6). The increase of (α) or (Re) leads to increase of centrifugal force and hence the kinetic velocity near the outer wall is decreased.

The effect of gap width on axial velocity is shown in Fig. (7), where it is clear that the increase of gap width leads to increase of (W) at the inner wall and decrease of (W) at the outer wall, so that the mean axial velocity is kept the same .

Pressure Distribution :

Figs (8 to 10)show the pressure distribution in the annular gap for different Reynolds number,injection angle and gap width . The effect of (α) is shown in Fig(8). The higher the injection angle the lower the value of the pressure drop at the inner wall and the higher is the value at outer wall . This would possibly occur due to the expected increase in centrifugal forces with increase in both (Re) and (α).

Fig.(9) shows the effect of Reynolds number on the pressure drop along the flow . It is seen that at high values of Reynolds numbers higher pressure drops are existed on the inner wall which can be ,again , a result of an increase in the centrifugal force .

Concerning the effect of the gap width,as can be seen from fig.(10), the larger the gap width (N is smaller) the lower is the computed pressure drop, a result which is quite expected .

Coefficient of friction (f):

Predictions of the coefficient of friction are shown on Figs.(11 to 13). It can be seen from fig.(11) that along the annular space (f) is decreasing. The effect of injection angle on the coefficient of friction in the entrance section (up to $Z \leq 8$) differes from its effect at $Z > 8$. At $Z \leq 8$ increase of (α) results in a corresponding increase in the frictional losses .At $\alpha = 80$ (f) is very small due to a propable reverse flow. At $Z > 8$ and $\alpha < 80$ the variation in injection angle has no but a slight effect on the coefficient of friction .

It is also seen in fig.(12) that increasing (α) ($Z = 4$, $N = 0.5$) leads to a slight increase in the coefficient of friction compared to the corresponding increase at higher Reynolds number up to $\alpha = 65°$, where at $Re = 3000$, a possible reverse flow would have the effect of reducing the coefficient of friction . The increase of Re, as expected, leads to lower values of (f). The effect of the gap width on (f) is shown on fig.(13). The higher the value of the gap width the higher to the coefficient of friction as would be expected due to the lesser rate of swirl decay in large annuli .

Temperature distribution and nusselt No(Nu):

Theoretical predictions of the temperature distribution in the annular gap is shown in figs (14 to 16). It is clear from these figures that the increase in either Reynolds number, α , or gap width increases the temperature across the flow at corresponding sections. This can be expected since increase of Re or α decreases the thermal boundary layer thickness . As to the increase in gap width the effect in increasing temperatures would be the longer contraction of motion .

The results of Nusselt number are shown in Figs (17 to 19). Concerning the effect of (α) at $Z \leq 8$, according to Fig 17, Nu increases as (α) increases, but at $Z > 8$ Nu decreases to a nearly constant value. In case of $\alpha = 80°$ the Nusselt number decreases along the annular space .
Fig.(18) shows (Nu) versus (α) at different Re. Increase of Reynolds number leads to increase in Nusselt number. The rate of increase in Nusselt number at constant Reynolds number is higher at $\alpha \geq 60°$. The increase in gap width increases Nusselt number as can be seen in fig 19. Nusselt number results are correlated with the aforementioned results of temperature distribution .

Conclusions :

1) The tangential component of velocity decays faster along the annular gap in case of smaller gap widths. This has the effect of reducing the coefficient of friction for smaller gaps swirling annular flow .

2) Higher rates of heat transfer are expected to occur at higher values of injection angle ($Z \leq 8$),while the rate decreases at values of $Z > 8$. It is therefore recommended to utilize the decaying swirl flow in annular spaces in relatively shorter (or compact) heat exchangers.

3) In a swirling flow through an annular space, the friction coefficient decreases with increase in Reynolds number while on the contrary Nusselt number increases with increase in Reynolds numberat a given injection angle and gap width .

REFERENCES:

1) Talbot,L.,
" Laminar swirling flow", ASME,Trans.(J.App. Mechanics) Vol.21,March, 1953 .

2) Kreith,F.,and SOnju,O.K.,
"The decay of turbulent swirl in a pipe",Journal of fluid Mech.,Vol. 22,Part 2,1965,PP.257-271.

3) Rochino,A.,and Lavan,Z.,
"Analytical investigations of incompressible turbulent swirling flow in stationary Ducts" , transactions , ASMEn,June. 1969,PP. 151- 158.

4) Yajnik,K.S.,and Subbaiah,M.V.,
J.Fluid Mech.,Vol.60, Part 4,1973,P.665.

5) Seno,Y.,and Negata,T.,
Trans.Japan soc.Mech.Engrs.,Vol.38,No 308 , 1972 - 4, P. 759.

6)Taylor,G.I.,
"Stability of a viscous fluid between two rotating cylinders with axial flow",Philosophical transactiong, Royal society,London, Series A,Vol.223, 1923,PP. 196 - 343.

7) Scott,C.J.,and Rask,D.R.,
"Turbulent viscosities for swirling flow in a stationary annulus",J.Fluid Eng.,ASME,Dec, 1973, PP. 557 - 566 .

8) Coney,J.E.R., and Simmers,D.A.,
"The effect of Taylor vortex flow on the development length in concentric annuli",
J.Mech.Engng Sci. Vol.21, No.2, 1979 ,
PP. 59 - 64 .

APPENDIX (A)

Example to use finite difference representation

Finite difference representation of the tangential boundary layer equation :

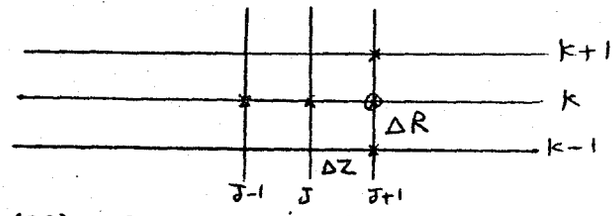

Fig.(20)grid points involved in the difference representation

Replacing the derivatives in equation (2-c) by the following finite difference approximations.

$$\frac{\partial v}{\partial r} = \frac{V_{J+1,K+1} - V_{J+1,K-1}}{2\Delta R}$$

$$\partial^2 v/\partial r^2 = \frac{V_{J+1,K+1} - 2V_{J+1,K} + V_{J+1,K-1}}{\Delta R^2}$$

$$\partial^2 V/\partial Z^2 = \frac{V_{J+1,K} - 2V_{J,K} + V_{J-1,k}}{\Delta Z^2}$$

$$\text{and } \partial v/\partial Z = \frac{V_{J+1,k} - V_{J,k}}{\Delta Z}$$

The equation(2-c) to a linearized finite-difference form becomes .

$$u_{J,K}\left[\frac{V_{J+1,k+1} - V_{J+1,k-1}}{2\Delta R}\right] + \frac{U_{J,k}.V_{J+1,k}}{(R)_k} + W_{J,k}\left[\frac{V_{J+1,k} - V_{J,k}}{\Delta Z}\right]$$

$$= \frac{2(1-N)}{R_e}\left[\left[\frac{V_{J+1,k+1} - 2V_{J,k} + V_{J+1,k-1}}{\Delta R^2}\right] + \frac{1}{R(k)}\left[\frac{V_{J+1,K+1} - V_{J+1,k-1}}{2\Delta R}\right]\right.$$

$$\left. + \left[\frac{V_{J+1,k} - 2V_{J,k} + V_{J-1,k}}{\Delta Z^2}\right] - V_{J+1,k} / R^2(k)\right] .$$

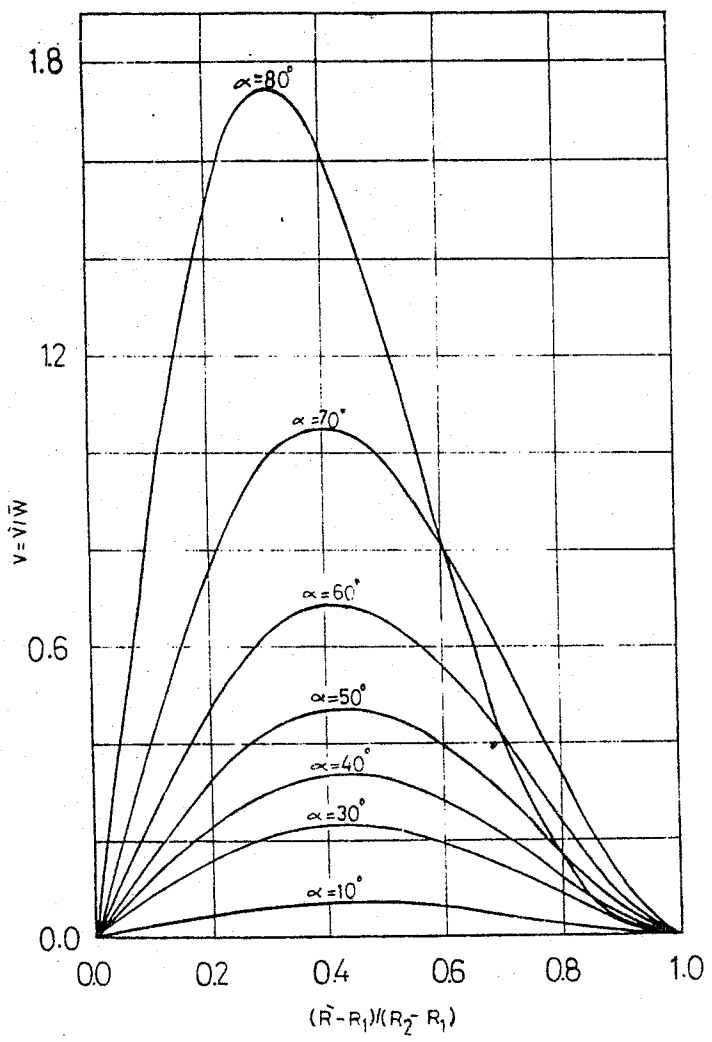

Fig. 2 :Effect of(α) on the tangential velocity

(R_e =1000 N=0.5 Z=4)

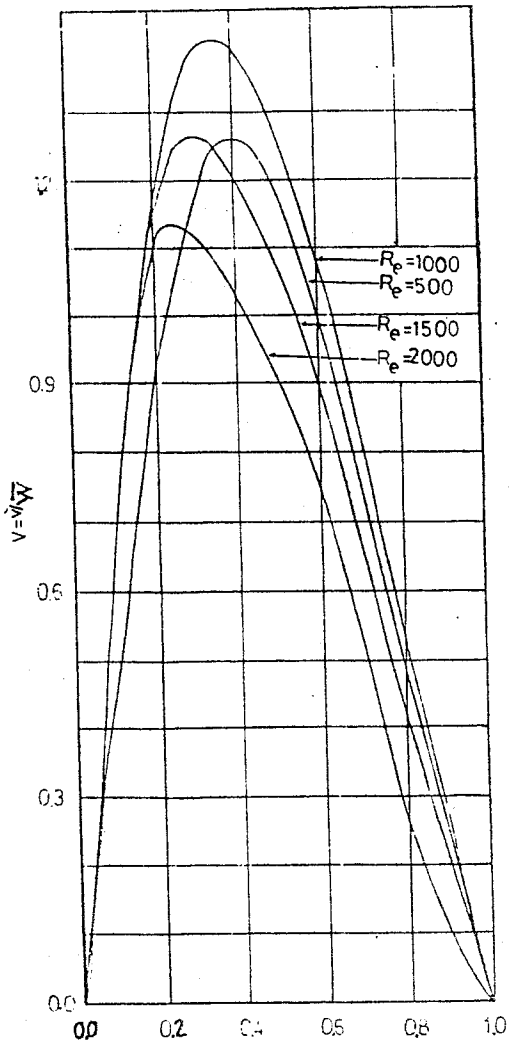

Fig. 3 Effect of (R_e) on the tangential velocity

(α = 80° N = 0.5 Z = 8)

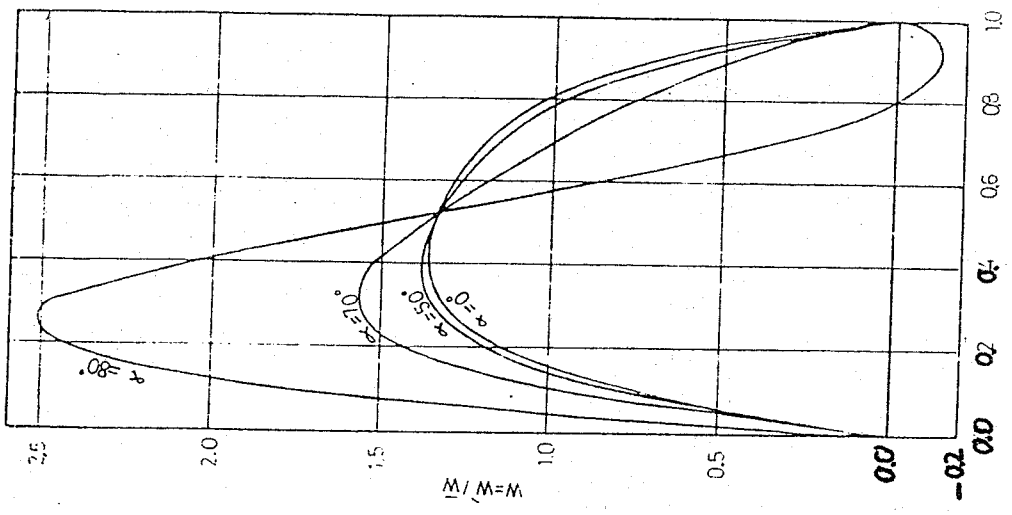

Fig. 5 Effect of (α)on the axial velocity
(R_e =1000 N=0.5 Z =0)

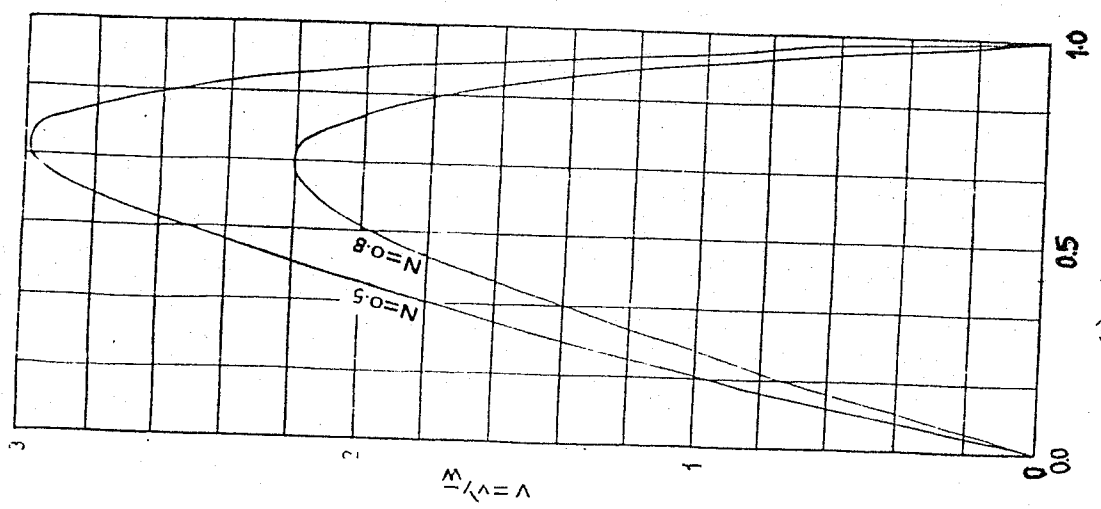

Fig. 4 Effect of (N) on the tangential velocity
(R_e= 1000 Z=0 α = 80°)

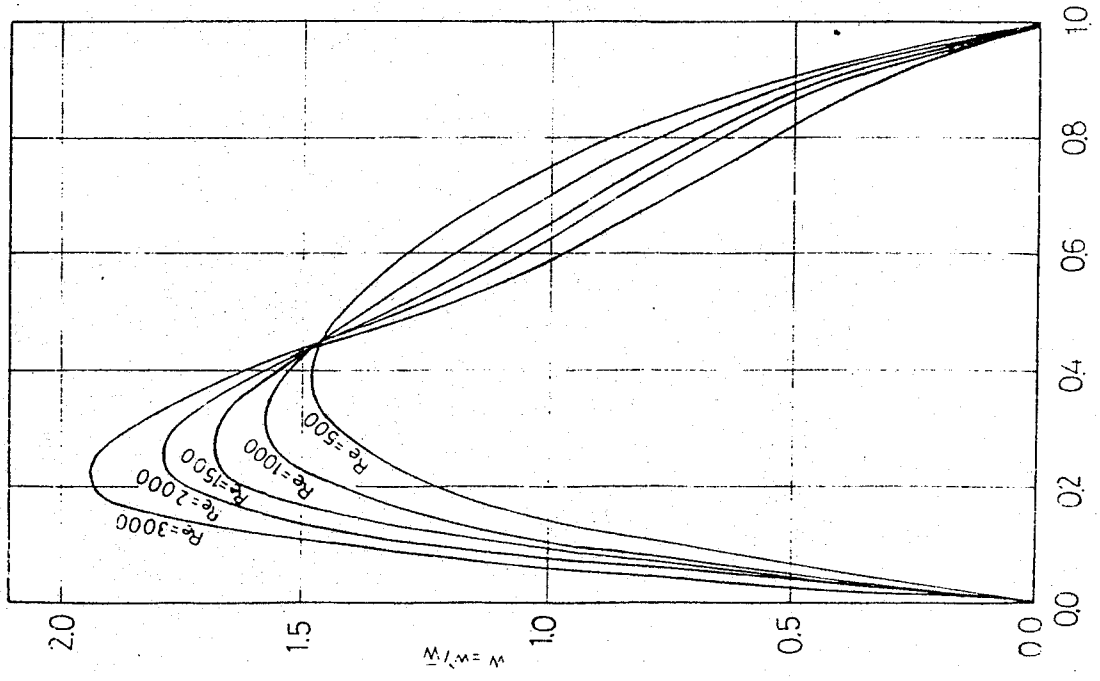

Fig. 6 : Effect of (R_e) on axial velocity profiles

(α=70° N=0.5 Z=0)

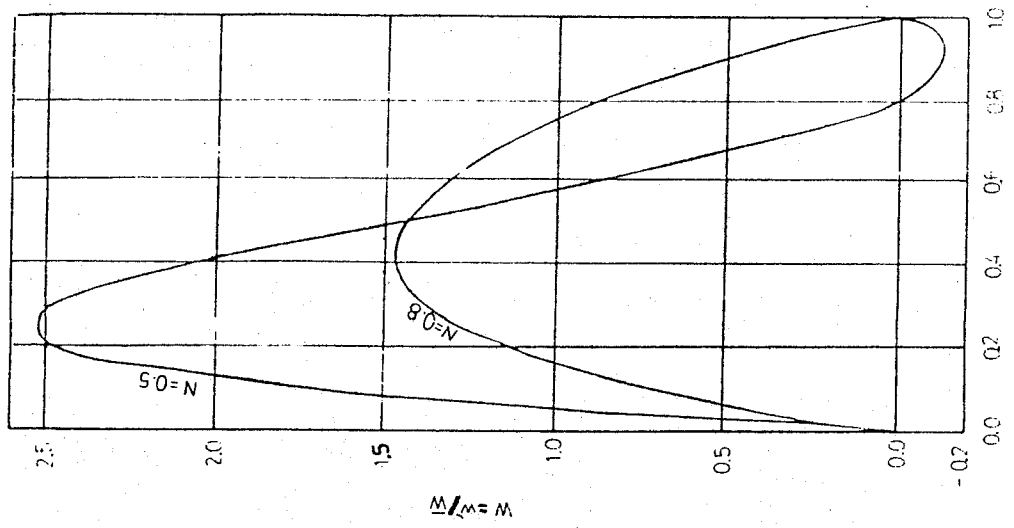

Fig. 7 : Effect of (N) on the axial velocity profiles

(R_e =1000 Z= 0 α =80°)

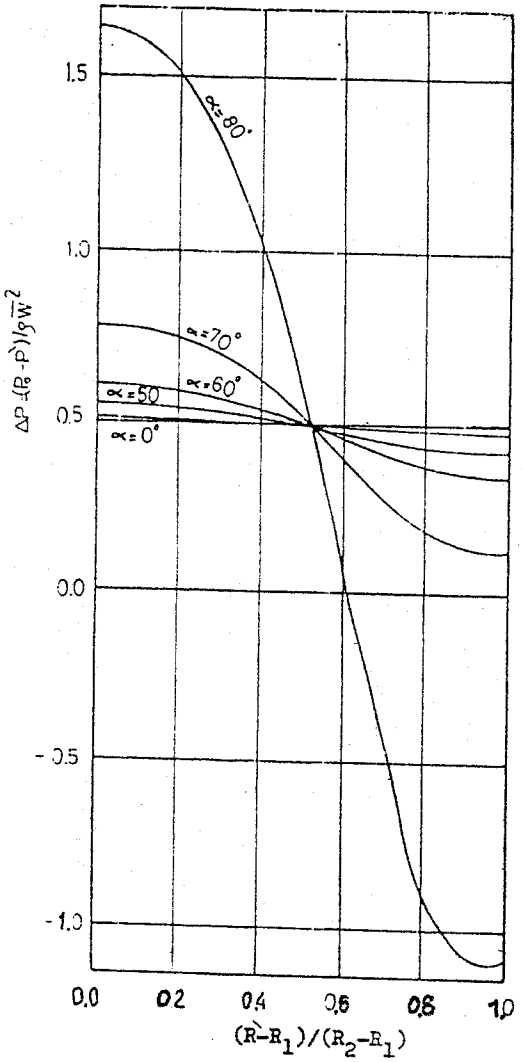

Fig. 8 Effect of (α) on pressure distribution

(R_e =1000 N =0.5 Z =0)

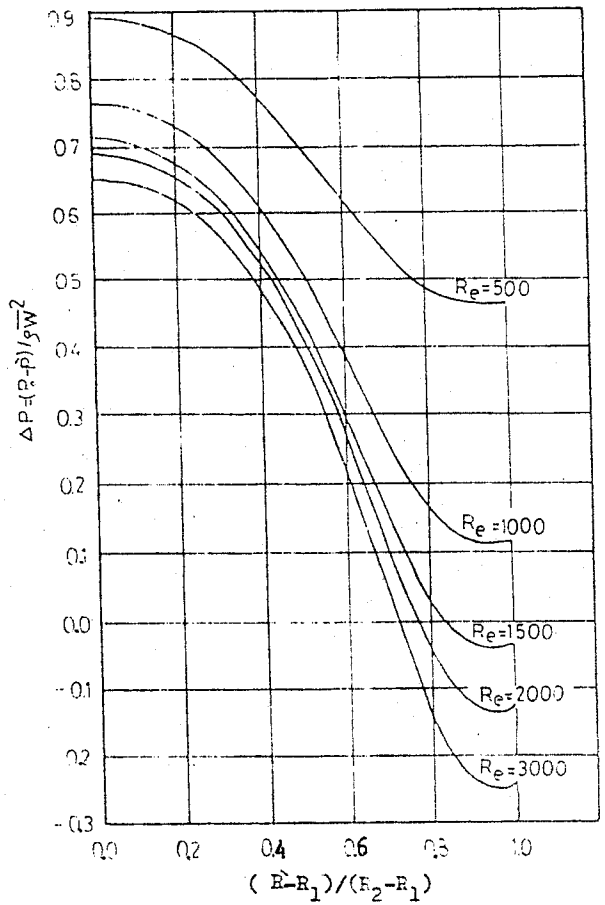

Fig. 9 Effect of (R_e) on pressure distribution .

(α =70° Z= 0 N=0.5)

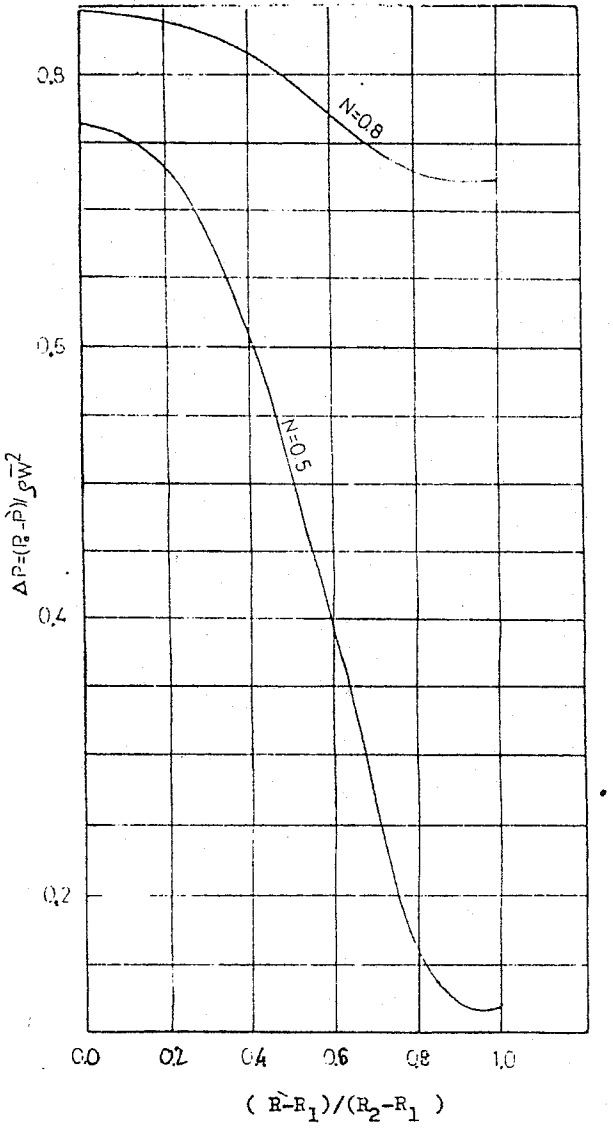

Fig. 10 Effect of (N) on pressure distribution .

(R_e =1000 Z = 0 α = 70°)

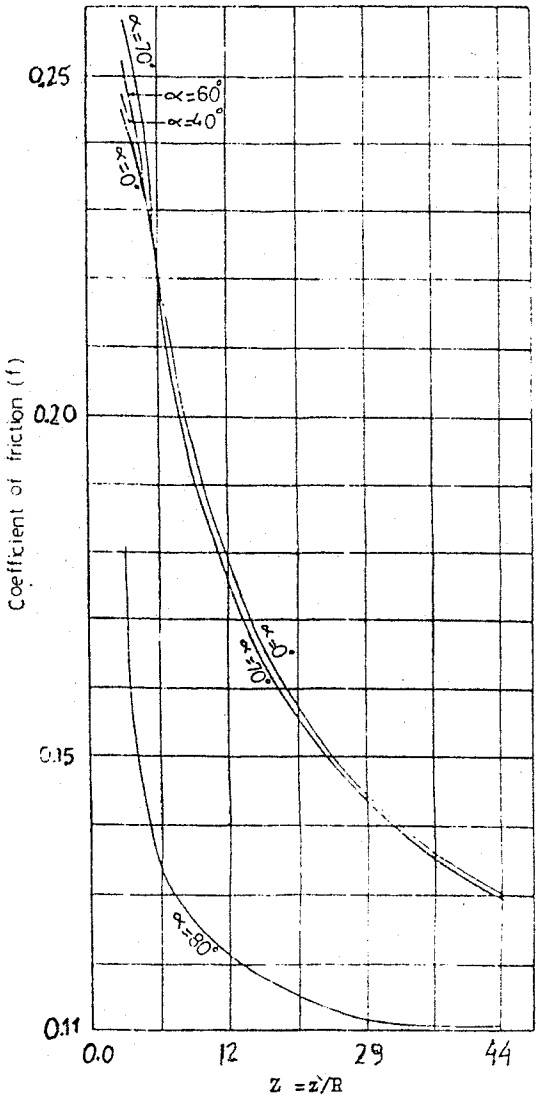

Fig. 11 Effect of (α) on coefficient of friction .

(R_e= 1000 N = 0.5)

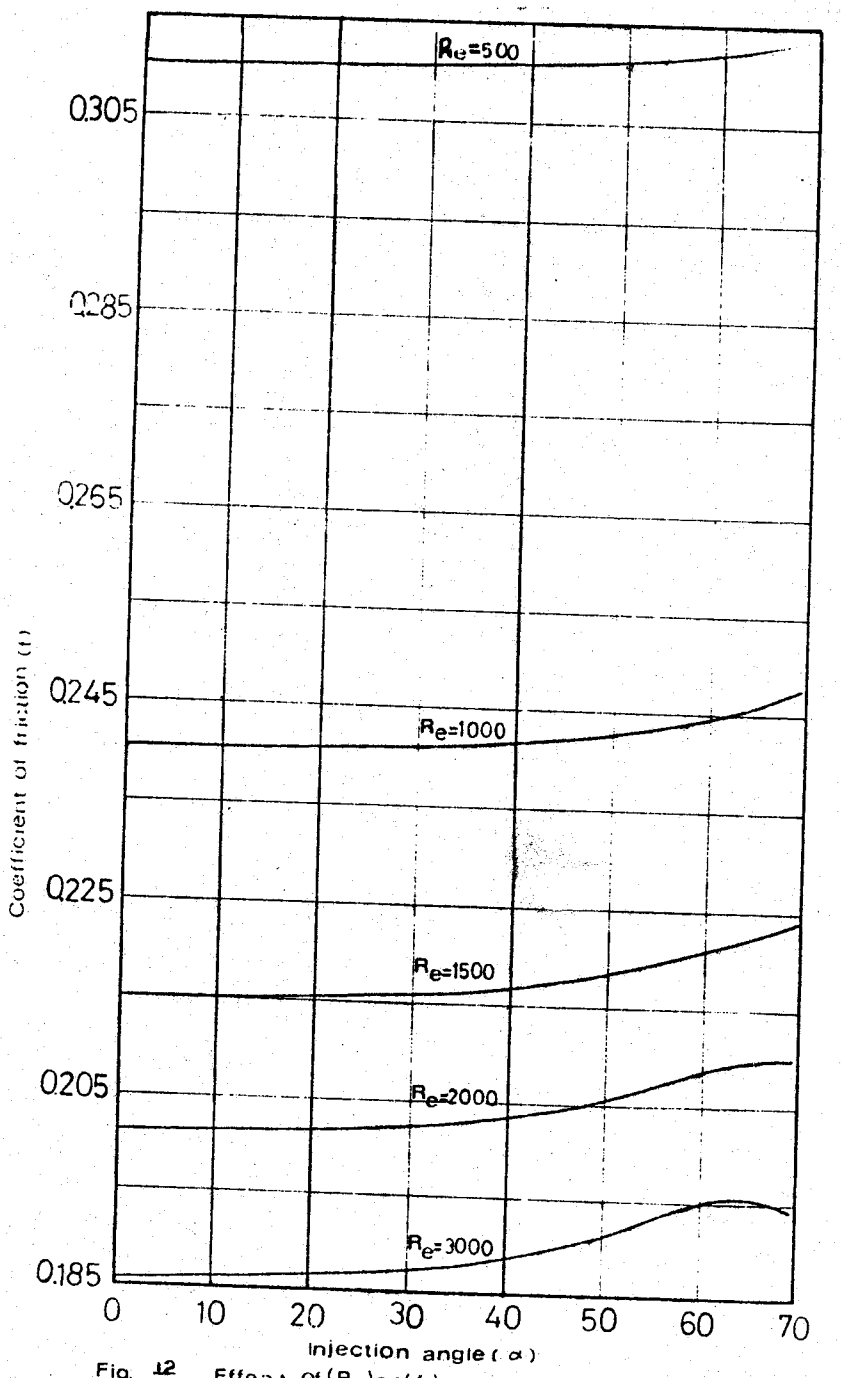

Fig. 12 Effect of (R_e) on (f.)

(Z=4 N=0.5)

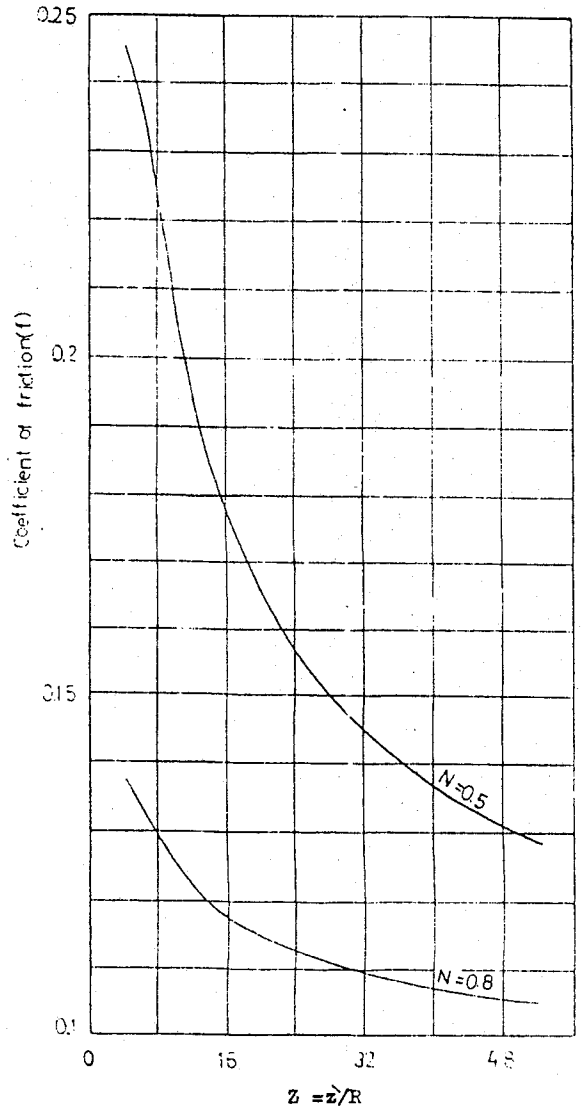

Fig. 13 Effect of (N) on coefficient of friction .

(R_e = 1000 $\propto$ =0 °)

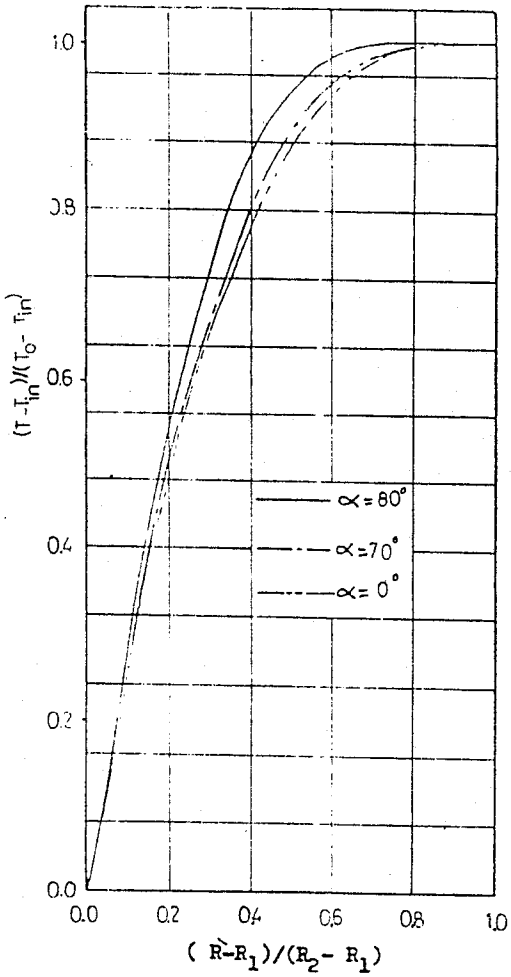

Fig. 14 Effect of($\propto$) on temperature distribution .

(R_e = 1000 Z =4 N =0.5)

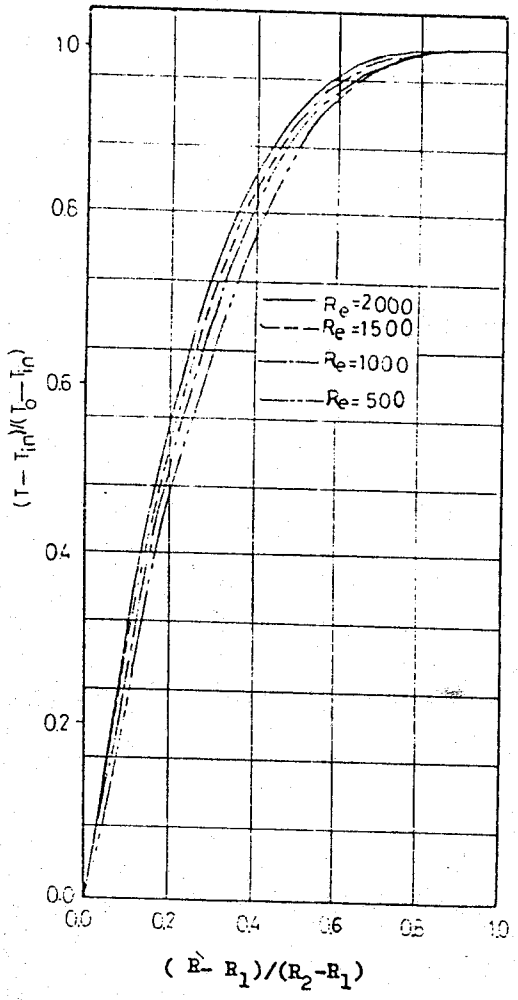

Fig. 15 Effect of (R_e) on temperature distribution .

(α= 70° Z =4 N= 0.5)

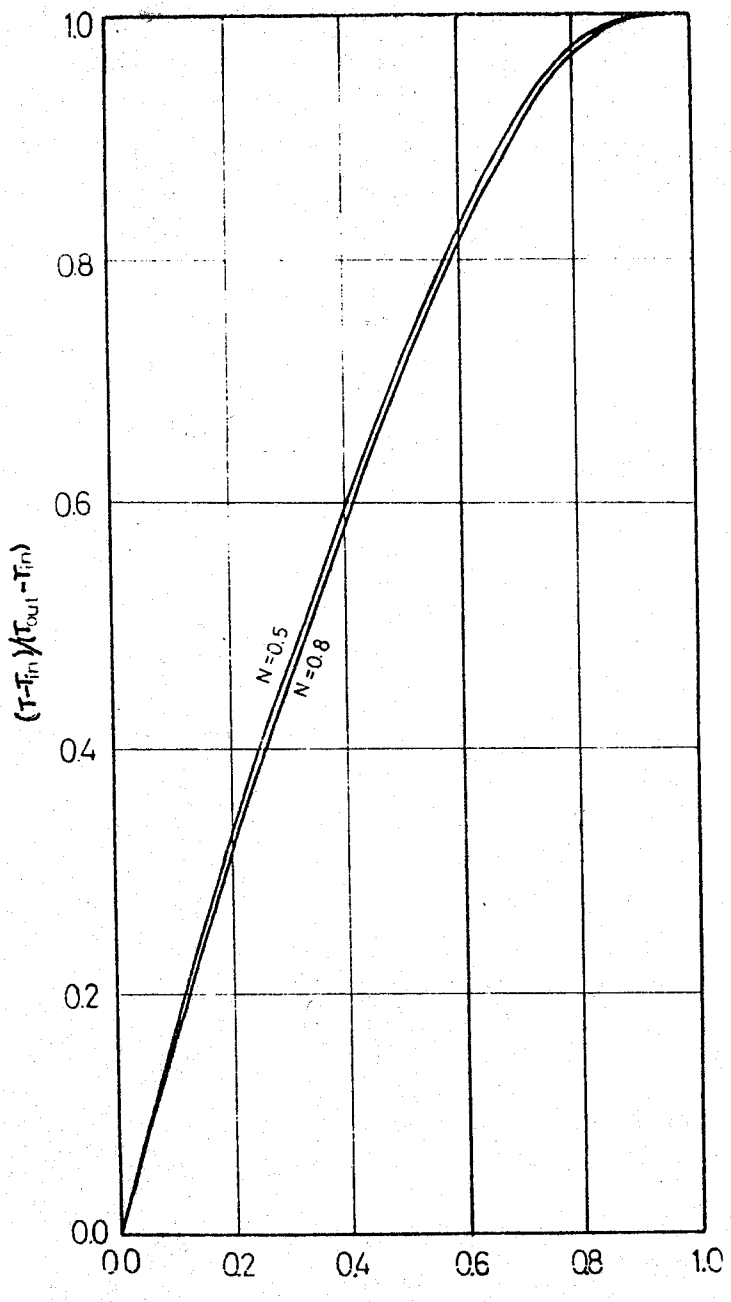

Fig. 16 Effect of (N) on temperature distribution
(R_e=1000 Z=0 α=80°)

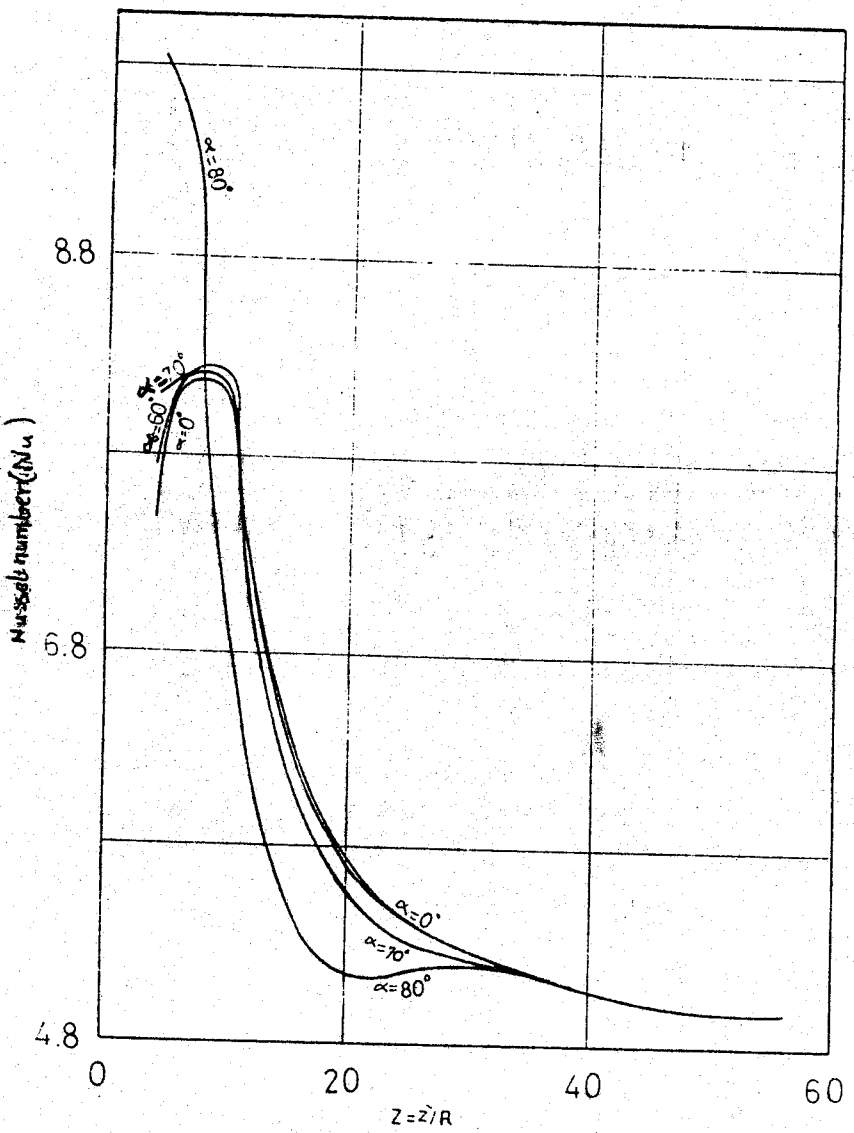

Fig. 17 :Effect of (α) on (N_u)

(R_e=1000 N=0.5)

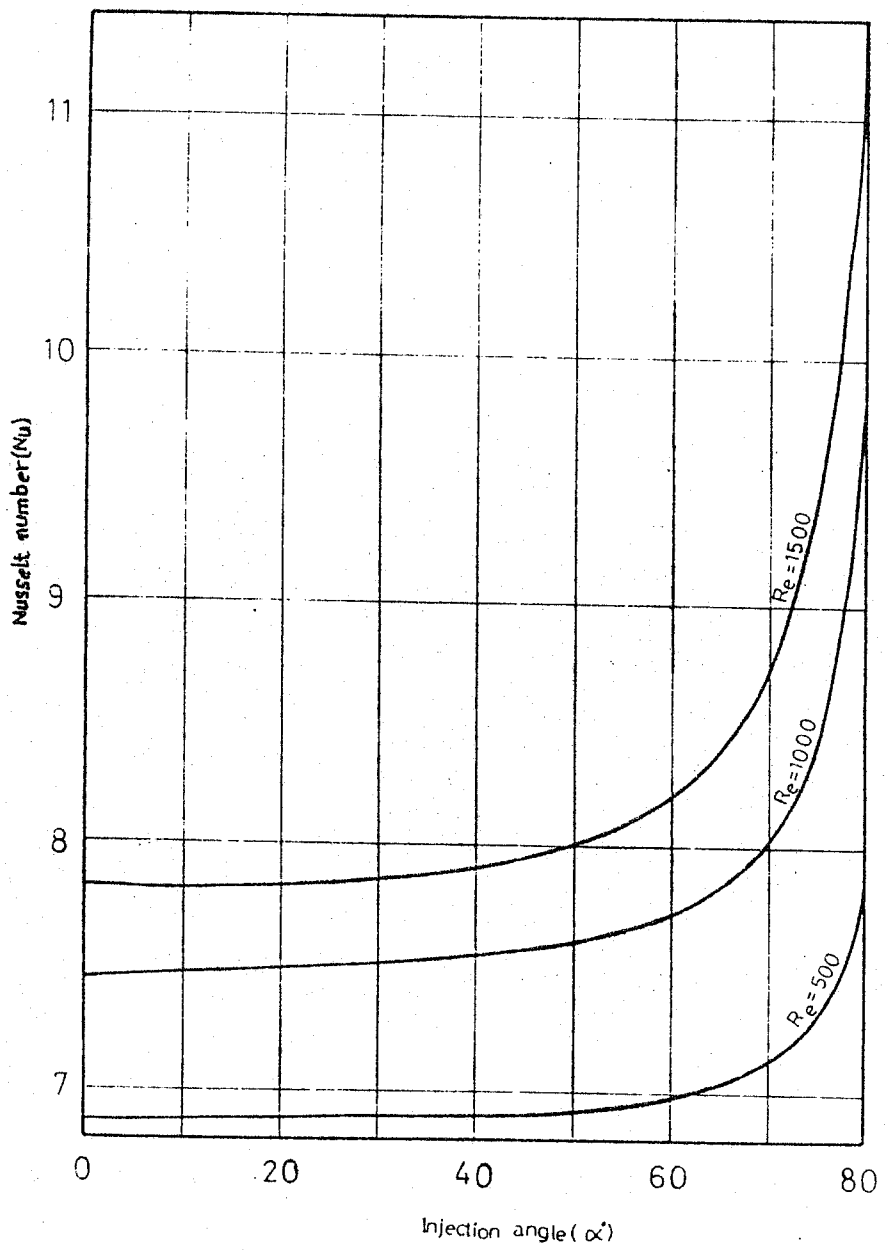

Fig. 18 :Effect of (α) on (N_u) at different (R_e)

(Z=4 N=0.5)

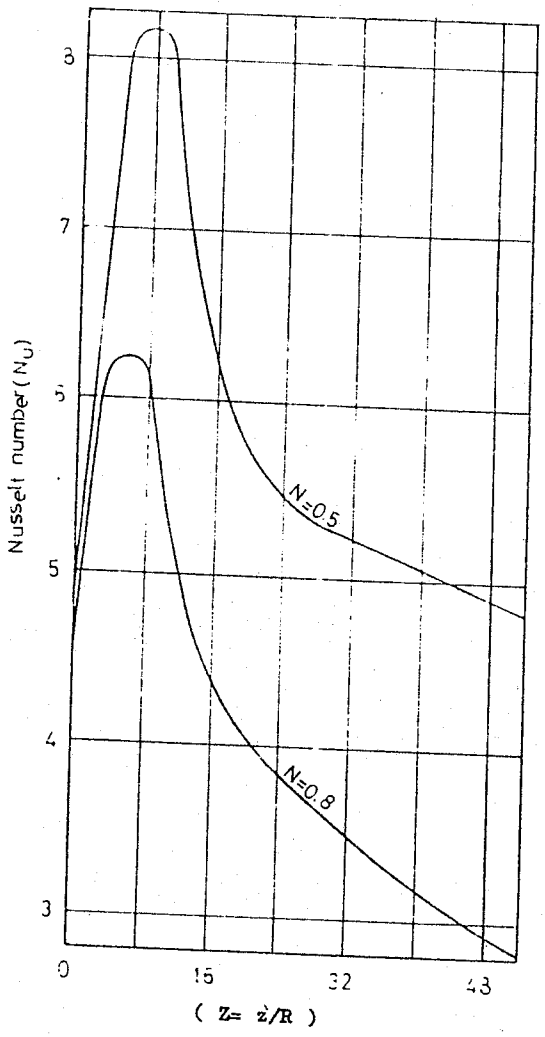

Fig. 19 : Effect of (N) on Nusselt number (Nu).
(R_e = 1000 α =0°)